CONF-880812--25

EXPERIMENTAL STUDY OF FLUX PINNING IN NbN FILMS AND MULTILAYERS:

ULTIMATE LIMITS ON CRITICAL CURRENTS IN SUPERCONDUCTORS*

K. E. Gray, R. T. Kampwirth, D. W. Capone II,** and J. M. Murduck†

Materials Science Division, Building 223

Argonne National Laboratory, Argonne, Illinois 60439 U.S.A.

Submitted to the 1988 Applied Superconductivity Conference,
San Francisco, CA, August 21-25, 1988

August 1988

CONF-880812--25

DE89 003622

*Work supported by the U.S. Department of Energy, BES-Materials Sciences, under contract #W-31-109-ENG-38.

**Present address: Supercon, Inc., Shrewsbury, MA.

†Present address: TRW, Redondo Beach, CA.

EXPERIMENTAL STUDY OF FLUX PINNING IN NbN FILMS AND MULTILAYERS: ULTIMATE LIMITS ON CRITICAL CURRENTS IN SUPERCONDUCTORS

K.E. Gray, R.T. Kampwirth, D.W. Capone II* and J.M. Murduck**

Materials Science Division, Argonne National Laboratory, Argonne, IL 60439

ABSTRACT

A flux pinning model is presented which predicts the maximum critical current density attainable in superconductors. That such a limit must exist comes from the realization that flux pinning is strongest in regions of weak superconductivity, but these regions cannot carry a large supercurrent. Since the same regions within the superconductor cannot be used for both pinning and supercurrent conduction, there must be an optimum mix, leading to a maximum J_c. Measurements on films and multilayers of NbN have verified many details of the model including anisotropy effects and a strong reduction in J_c for defect spacings smaller than the flux core diameter. In an optimized multilayer the pinning force reached ~22% of the theoretical maximum. The implications of these results on the practical applications of NbN films and on the maximum critical current density in the new high temperature superconductors are also discussed.

INTRODUCTION

The analysis of flux pinning in superconductors is a very complex subject, and difficulties in achieving adequate experimental conditions to test even the simplest models have limited progress in the field[1]. Even when the problems associated with the statistical summation of pinning centers are ignored, an estimate of the maximum attainable critical current density, J_c, has not been given. That such a limit must exist comes from the realization that flux pinning is strongest in regions of weak superconductivity, but these regions cannot carry a large supercurrent. Since the same regions within the superconductor cannot be used for both pinning and supercurrent conduction, there must be an optimum mix, leading to a maximum J_c. Many applications of superconductors, high-temperature as well as conventional, depend crucially on large values of J_c, so it would be particularly useful to be able to predict the maximum realizable pinning force and critical current density, J_c, for any arbitrary superconductor. In a recent paper[2], we began to suggest this possibility, through experimental measurements on samples with a well-defined geometry and pin distribution. These conditions were achieved by using thin NbN films exhibiting columnar grains, with ultra-thin insulating boundaries *perpendicular* to the film surface, and multilayers of NbN alternated with ultra-thin insulating AlN barriers, which provide a closely-spaced, regular array of pinning layers *parallel* to the film surface. The very strong pinning found for these extended defects has the additional advantage that it effectively destroys the regular flux lattice, thus removing the necessity to consider the complications associated with statistical summations of the pinning forces.

Manuscript received August 22, 1988.

The results of this study[2] showed a ubiquitous field dependence for J_c of $(1\text{-}b)^2$, where $b \equiv B/B_{c2}$ and B_{c2} is the upper critical field. Previously, this field dependence had been universally identified with flux flow resulting from shearing of the flux line lattice[3], but in the present case of the multilayers in a parallel field, shearing past the AlN insulating layers is impossible. Thus the $(1\text{-}b)^2$ dependence has been clearly demonstrated for cases which cannot exhibit shear, and we must seek another explanation.

As a reasonable starting point, we proposed[2] a planar vacuum interface model of the flux pinning, in which the pinning force is given by the difference in free energy, E_c, between the superconducting and normal states (proportional to $(1\text{-}b)^2$) divided by the coherence length ξ. Kes[4] has pointed out that this E_c is a spatially averaged quantity, whereas the pinning force should depend on local gradients of the free energy. Such gradients[5] include a derivative of the order parameter which has a field dependence proportional to (1-b), and would thus always dominate for fields close to B_{c2}. The lack of this dependence in the experimental results could be caused by the finite insulator width (~1.5-2 nm) of the grain boundaries and AlN layers. In such circumstances, the order parameter is not required to vanish in a singularity at the vortex center and thus the derivative of the order parameter may be significantly smaller than in the case of usual grain boundary or point defect pinning. For example, the usual analysis of Josephson junctions in a parallel field takes the order parameter as constant right up to the insulating barrier. As a result the (1-b) term may be negligible. There is a need for a more complete theoretical description of these finite-width, extended pinning structures which must include the Josephson coupling of the superconducting wave function across the insulating boundary.

Similar experimental results, obtained by Pruymboom, et al[6] for very thin NbN films in perpendicular fields, have been interpreted as due to shearing of the flux lattice. These authors outlined a model which reproduces the correct magnitude of J_c, providing the shear channel width is given by the flux line spacing at $B=B_{c2}$. In this model the pinning has relatively little to do with the detailed defect structure causing the pinning. For the thicknesses of films used in their study, the average grain diameter did not change appreciably. Our measurements, covering a wide range of average grain diameters and multilayer spacings, showed a strong dependence of J_c on defect spacing (see Fig. 4), which was indistinguishable between the perpendicular field results, and those for multilayers in parallel fields for which shear is impossible. Thus, while we cannot unambiguiously rule out a shear mechanism for the perpendicular fields, the experimental evidence seems to favor the same mechanism for both field orientations.

The combined results in our sputtered single and multilayer NbN films show a surprising similarity for both field orientations. The J_c increases linearly with defect concentration, followed by a dramatic drop when the spacing of the pinning centers is of order of the flux core diameter or less. This result, together with our theoretical model, provides a definitive upper limit on J_c which can be readily evaluated, and is shown to be less than the critical depairing current density.

These studies are also of interest because NbN films show potential as conductors for high-field superconducting magnets, especially for fusion, because of their excellent high-field superconducting properties[7-9] and tolerance to radiation[10] and strain[11]. For magnet applications, it is $J_{c\parallel}$, i.e., with the field parallel to the film surface which is most relevant. Therefore, another goal of this research is to test methods to increase $J_{c\parallel}$ of NbN beyond its previous limiting value[8,9] of $\approx 10^4$ A/cm^2 for 3 μm thick films in a 20 T field, and to understand how to achieve these results in films of practical thicknesses (20-50 μm) for high-field magnets.

Finally, since the anisotropies and ratios of layer spacing to superconducting coherence length, ξ, of the NbN multilayers are analogous to the conducting Cu-O planes of HTS, e.g., $YBa_2Cu_3O_7$, we are able to predict potential maximum J_c values for the latter.

EXPERIMENT

Sample Preparation and Characterization

Samples were prepared on polished sapphire substrates using magnetron reactive sputtering[8] with a mixture of Ar and N gases. Substrate temperatures were maintained at ≈300°C and deposition rates between 4-5 nm/sec. To evaluate the effect of grain diameter and film thickness on J_c, a series of films of thickness between 0.14 μm and 10 μm were prepared under similar sputtering conditions, which were chosen to optimize the high-field properties, based on previous work[8].

The transition temperature as a function of field was determined from an extrapolation of the midpoint of the resistive transition to zero resistance for fields up to at least 6 T. The film transition temperature, T_c, was determined from the zero-field intercept of a linear-least-squares-fit of this data, so that T_c was representative of the finite field properties of the films. Temperatures were measured to an accuracy of ±0.1 K using a carbon glass thermometer. For individual films, the values of T_c ranged from 13.4 K for the thinnest film to 14.5 K for the 10 μm film.

Transmission electron microscopy (TEM) studies of Ho, et.al.[12] showed that NbN films prepared under a variety of sputtering conditions exhibited a universal relationship between average diameter, $\langle d \rangle$, of the columnar grains and the distance, t, above the film/substrate interface. A typical example exhibits columnar grains growing perpendicular to the substrate. For films prepared in our laboratory, we find:

$$\langle d \rangle \approx 6\ \mathrm{nm} + 0.05t, \qquad (1)$$

yielding conical grains with an average grain diameter, throughout the film thickness, of ≈ 80 nm for 3 μm thick films. As such, a reduction of the average NbN grain diameter is readily accomplished by reducing the film thickness. We have shown (see Fig. 1a) that decreasing the film thickness to 0.14 μm increases the value of $J_{c\perp}$, i.e., *with the field perpendicular to the film surface, however,* it has little or no effect on $J_{c\parallel}$. The latter result is understood to be because the columnar grain boundaries are approximately perpendicular to the flux lines in that case, and are thus ineffective as pinning centers.

Although grain boundaries parallel to the film surface have not been realized, pinning due to film surfaces can improve $J_{c\parallel}$. We have shown that such effects are of limited consequence for films which are much thicker than $\xi \approx 4$ nm. However, in the limit of extremely thin NbN layers (≈10 nm), which are necessarily sandwiched between layers of another material to prevent oxidization, the surfaces are shown to be very effective at increasing $J_{c\parallel}$. In the cases studied here[13], insulating AlN layers of thickness 2 nm are alternated between NbN layers of various thicknesses, and such samples show significant increases in $J_{c\parallel}$.

Multilayer samples were fabricated using an oscillating substrate plate which was programmed to position the substrates over either of two sputter guns, with Nb and Al targets, for the period of time necessary to build each layer. The deposition rate was about 2 nm/sec. Aluminum nitride was chosen[13,14] because it can be formed by reactive sputtering with N, just as NbN is, and it has a lattice constant close to that of NbN. It was found necessary to carefully control the N partial pressure, which *was the same* for both layers[14]. The multilayers, which consisted of 2 nm AlN barrier layers alternated with NbN layers of thicknesses between 4 and 35 nm, exhibited T_c values between 9.6 and 13.6 K.

Note that the grain boundaries of single NbN films, unlike usual metals, are ≈1.5 nm thick[12], and presumably insulating to account for the very high transport resistivity[7-9]. Thus for comparison purposes the grain boundary pinning should closely approximate that of the 2 nm AlN layers.

Critical Current Densities

In all cases, J_c is defined by the current which results in an electric field of 1 μV/cm. Measurements of $J_c(H)$ above 6 T were made at the Francis Bitter National Magnet Laboratory. Measurements of J_c for both parallel and perpendicular field orientations have been done for single films as a function of thickness and for multilayers as a function of the NbN layer thickness. These have been reported in greater detail in Ref. 2. Since different flux pinning models predict J_c proportional to (1-b) as well as $(1-b)^2$, we have plotted our data against $(1-b)^n$, and varied n to get the smallest deviations in the fit. In such tests, the best fits occur for $n \sim 1.85$ to ~ 2.2, with random spread which is presumably due to inhomogeneities in the films and scatter in the experimental data. It thus seems reasonable to choose n=2 and plot the data in a manner which allows us to extrapolate to B_{c2}. Plots which demonstrate the $(1-b)^2$ behavior of $J_{c\perp}$ and $J_{c\parallel}$ are shown in Fig. 1 for both single NbN films and multilayers. Note that J_c is also normalized by the superconducting condensation energy per unit volume, $B_c^2/2\mu_o$, so the effects of varying T_c are removed and the slopes of these plots reflect the true, bare pinning force of the defects. In all cases, B_c has been estimated from the measured value of 0.234 T for bulk samples[15], by scaling it linearly with the ratio of T_c measured in our films to the 15.54 K value of the bulk sample[15].

Several additional comments are necessary here. Note that the $(1-b)^2$ dependence of J_c is not restricted to only NbN. It is found in the A-15 superconductors[1] like Nb_3Sn and Nb_3Ge, high temperature superconductors[16] like $YBa_2Cu_3O_7$ and even NbTi alloys[17]. The latter case is not so obvious and, in fact, many have concluded that the dependence goes as (1-b). However fairly close to B_{c2} the dependence is seen to be well-described by $(1-b)^2$. Figure 2 shows a representative example of data on various alloys of NbTi measured by Larbalestier[17].

Finally, note that the destruction of the regular flux line lattice in NbN is borne out by a lack of evidence of a modulation of $J_{c\parallel}(H)$ near B_{c2} for our well-defined multilayer structures. This modulation is expected to result from a matching condition between the regular multilayer spacing and the regular flux lattice spacing.

PLANAR VACUUM INTERFACE MODEL

We present a simple model which allows us to: determine the theoretical maximum pinning force, and hence J_c, which occurs for an ideal planar vacuum interface; to deal with the anisotropies found in our NbN samples and in the high-temperature superconductors (HTS), e.g., $YBa_2Cu_3O_7$; and to compare between the two dominant types of pinning centers in these samples. An analysis is required for two experimental situations: pinning by the film surfaces for parallel fields; and pinning by the columnar grain boundaries for perpendicular fields. In both cases, pinning by regularly spaced plane boundaries parallel to the vortices should be a reasonable approximation. We present a simple, calculable model for the pinning force of an *ideal planar vacuum interface*. To determine the pinning force for an individual flux line, the free energy of a flux line is needed. It is higher when located in the superconductor, because of the loss of superconducting condensation energy, by an amount

$$E_c = \pi \xi_j \xi_f l (B_c^2/2\mu_o) (1-b)^2/\beta_A, \quad (2)$$

where l is the length of the flux line and the potential anisotropy of the superconducting properties result in two different coherence lengths, both orthogonal to the flux line. For later convenience, we choose ξ_j to be directed along the component of the transport current J which is perpendicular to B, and ξ_f to be along the Lorentz force, J X B, and hence perpendicular to both J and B. The $(1-b)^2$ factor results from Abrikosov's[18] solution of the

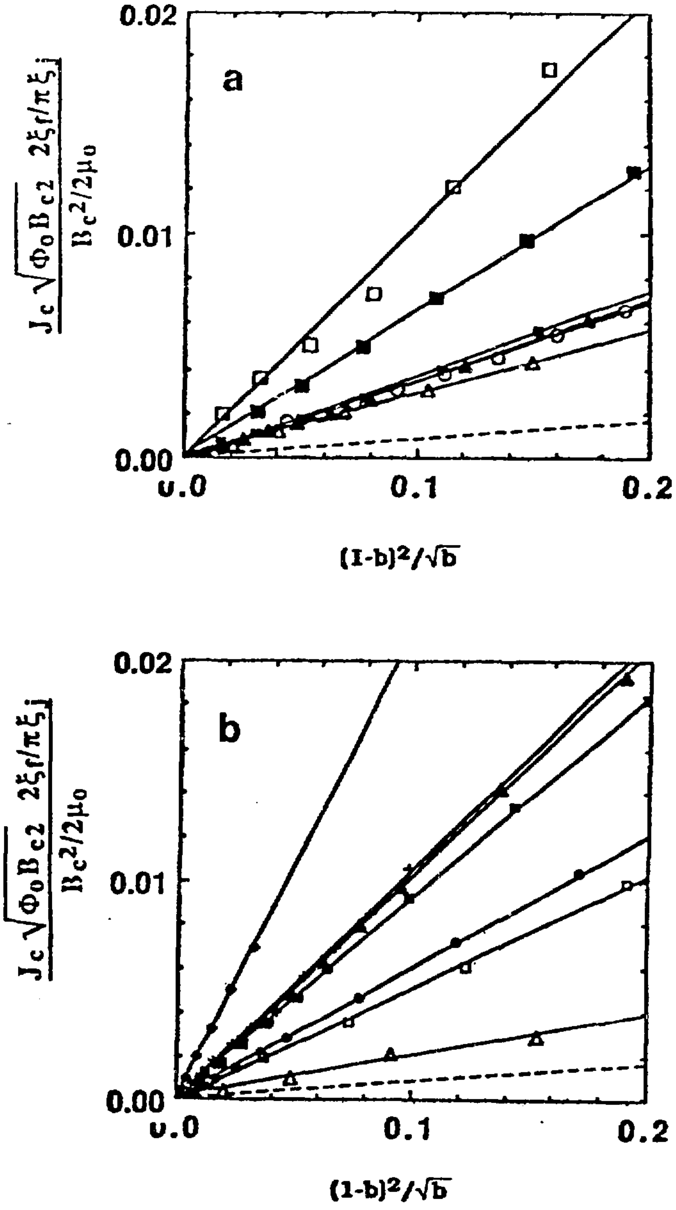

Figure 1. Most of the NbN data are plotted using a normalization described in the text, and $\xi_j/\xi_f=1$ and $\xi_j/\xi_f=B_{c2\parallel}/B_{c2\perp}$, respectively, for perpendicular and parallel fields. The linear-least-squares-fits are shown as solid lines. The slopes of these lines, S, are proportional to the bare pinning force after removing the dependence on T_c and B_{c2}. Also shown as the dashed line is the maximum limit of the Kramer flux shear model[3]. (a) Single NbN films for various thicknesses. Perpendicular fields: open squares, 0.14 μm; solid squares, 0.41 μm; and filled squares, 1.3 μm. Parallel fields: solid triangle, 0.14 μm; open circles, 0.41 μm; and open triangles, 1.3 μm. (b) Multilayers for various NbN layer thicknesses. Perpendicular fields: open squares, 26.3 nm; and open triangles, 13.1 nm. Parallel fields: plusses, 6.2 nm; solid diamonds, 10.5 nm; solid triangles, 13.1 nm; solid squares, 26.3 nm; and solid circles, 35 nm.

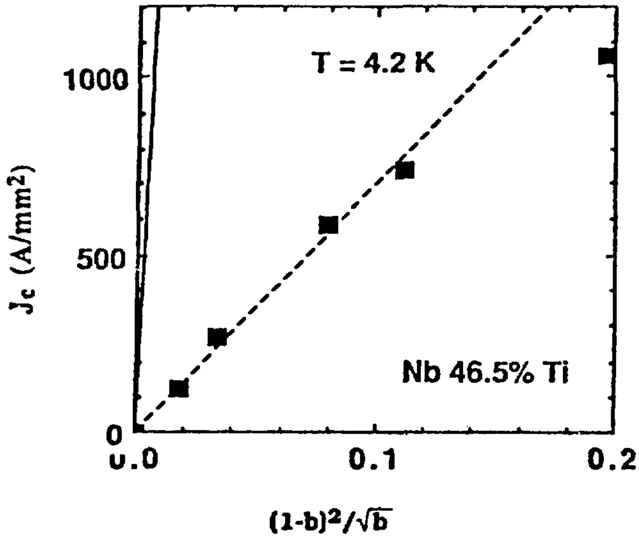

Figure 2. A representative example of J_c for NbTi alloys reported in Ref. 17 plotted against the reduced field variable as in Fig. 1. The dashed line is a guide to the eye and the solid line is the maximum value, J_{cm}, derived from the material properties of the NbTi alloy and the planar vacuum interface model.

Ginzburg-Landau equations near B_{c2}. Details of the flux line shape are contained in $\beta_A \equiv \langle\Psi^4\rangle/(\langle\Psi^2\rangle)^2$, where Ψ is the Ginzburg-Landau order parameter. For a triangular lattice, $\beta_A \sim 1.16$, but such details cannot be incorporated here (β_A is set equal to one in the following) because the pinning in our samples destroys the regular flux lattice.

Kes[4] has pointed out that this E_c is a spatially averaged quantity, whereas the pinning force should also depend on gradients of the *local* free energy. The local free energy includes[5] Ψ^4 which is proportional to $(1-b)^2$, and a derivative of the G-L order parameter, $\xi^2\nabla^2(\Psi^2)$, which has a field dependence proportional to (1-b). However, because of the finite insulator width (~1.5-2 nm) of the grain boundaries and AlN layers, the order parameter is not required to vanish in a singularity at the vortex center, and the derivative of the order parameter may be significantly smaller than in the case of usual grain boundary or point defect pinning. For example, the usual analysis of Josephson junctions in a parallel field takes the order parameter as constant right up to the insulating barrier. As a result the (1-b) term could be negligible, and the experimental results seem to verify this. For the same reason, it is difficult to *calculate* the precise gradient of pinning potential to arrive at the pinning force. An alternative explanation of the missing (1-b) term has been proposed by Kes[4]: the derivative term does not vary between regions with different T_c, such as alternating layers with a proximity effect or with different superconductors. This can be seen as a cancellation, with decreasing T_c, of an increase in ξ_o and a decrease in Ψ. However it is difficult to understand that the insulating layers in our experimental samples can be regarded as having a lower, but finite, T_c.

Until a more complete theory is developed, which must include the Josephson coupling of the superconducting wave function across the insulating boundary, we have adapted the usual treatment of dividing by the coherence length in the direction of the Lorentz force, i.e., ξ_f, so that:

$$f_p = E_c / \xi_f. \qquad (3)$$

The volume pinning force for a planar vacuum interface is then given by Eq. 4.18 of Ref. 19 as:

$$P_v = J_c B = (B/\Phi_o)^{1/2} f_p / dl, \qquad (4)$$

where d is the distance between interfaces and Φ_o is the flux quantum. Because of the simple geometry involved and the destruction of the regular flux lattice, there is no need to consider statistical summations over pinning centers, collective pinning models, etc., and the final result gives the critical *depinning* current density, J_{cv}, associated with an *ideal* planar vacuum interface as:

$$J_{cv} = \frac{2\xi_f}{d} \frac{B_c^2/2\mu_o}{\sqrt{\Phi_o B_{c2}}} \frac{\pi}{2} \frac{\xi_l}{\xi_f} \frac{(1-b)^2}{\sqrt{b}}. \qquad (5)$$

The redundant factors of ξ_f are left in the equation for the sake of clarity in later discussions of anisotropy, the experimental results and the ultimate limit of of J_c. It is important to note that Eq. 5 has the same field dependence as used above in Fig. 1 to fit the experimental data to determine B_{c2}. Therefore it is appropiate for analyzing the J_c data and the normalization used in Fig. 1 is readily understood: the slopes of the curves correspond to effective values of $2\xi_f/d$, indicating that the experimental J_c are always less than that of an *ideal* planar vacuum interface, J_{cv}.

For the cases considered in this paper, NbN films and multilayers and HTS, represented by current flowing in the Cu-O planes of $YBa_2Cu_3O_7$, the anisotropy factor is straightforward. In the plane of the NbN film (layers) or the Cu-O layers, the superconducting properties are reasonably isotropic resulting in superconductors with uniaxial anisotropy. Due to this approximate symmetry for directions parallel to the layers of NbN or in the a and b directions in $YBa_2Cu_3O_7$, there are only three distinct cases:

I. The parallel field case considered above, in which both B and J are in the NbN or a-b plane;

II. The perpendicular field case considered above in which B is along the film perpendicular or c-axis and J is in the a-b plane;

III. A new case, not readily accessable for thin films, in which B is in the a-b plane and J is along the c-axis.

It is easy to show that ξ_j/ξ_f in Eq. 5 is equal to ξ_a/ξ_c, 1 and ξ_c/ξ_a for these cases, where $\xi_a=(\Phi_o/2\pi B_{c2\perp})^{1/2}$ is the coherence length in the Cu-O or NbN film planes and $\xi_c=(\Phi_o/2\pi B_{c2||})^{1/2}(B_{c2\perp}/B_{c2||})^{1/2}$ is the coherence length perpendicular to the NbN or Cu-O layers[20]. As an example, case I gives a maximum potential critical depinning current density, J_{cm}, when $d=2\xi_f$, to be

$$J_{cm} = \frac{B_c^2/2\mu_o}{\sqrt{\Phi_o B_{c2||}}} \frac{\pi B_{c2||}}{2B_{c2\perp}} \frac{(1-b)^2}{\sqrt{b}}. \qquad (6)$$

A fundamental limitation on J_c, independent of the pinning strength, is the critical *depairing* current density, J_{cd}. This is readily calculated[21] with the Ginzburg-Landau theory to be $J_{cd}=4B_c/3\sqrt{6}\mu_o\lambda_L$, or, in a more transparent form for our use, $J_{cd}=16\pi\xi(B_c^2/2\mu_o)/3\sqrt{3}\Phi_o$. Then it is easy to find the ratio of maximum depinning to depairing critical current densities by using the $(1-b)^2$ factor for the condensation energy in J_{cd}. Assuming an isotropic case,

$$\frac{J_{cv}}{J_{cd}} = \frac{3\sqrt{6\pi}\ (2\xi_f/d)}{32\sqrt{b}} = \frac{0.407\ (2\xi_f/d)}{\sqrt{b}}. \qquad (7)$$

Since the maximum value of $2\xi_f/d$ is expected to be ~1 (see Fig. 4), we find that within the context of these models, depairing is not the ultimate limitation for fields b>0.2. However, note that the validity of extrapolating the models even below b~0.5 is questionable.

ANALYSIS OF NbN RESULTS

The results for single and multilayer films in perpendicular fields can be compared directly, since the extra surfaces will be ineffective pinning sites. In Fig. 3, the bare pinning forces, which are the slopes, $S_\perp$, of the Kramer-like plots of Fig. 1, are plotted against $2\xi_a$ divided by the average grain size, <*d*>, determined from Eq. 1. The most striking result is the sharp decrease in pinning force for values of <*d*> less than the flux core size, $2\xi_a$. This was anticipated on theoretical grounds, but is shown in striking fashion in Fig. 3. The maximum pinning force from Eq. 2 is shown as the solid line, and corresponds to the equality of the ordinate and abscissa values. A least-squares-fit to the first three data points is shown as the dashed line. Its slope is only 15% of the maximum pinning force, indicating a decreased effectiveness of the grain boundaries compared to an ideal vacuum interface. This could be due to the thinness of the insulating grain boundaries and the consequent Josephson coupling across them. Nonetheless, the intercept defines the strength of the *bulk* pinning force, *excluding grain boundaries and film surfaces*, as 0.024 in dimensionless units. This is equivalent to one maximum-pinning-force planar vacuum interface located every $2\xi_a/0.024 \approx 320$ nm.

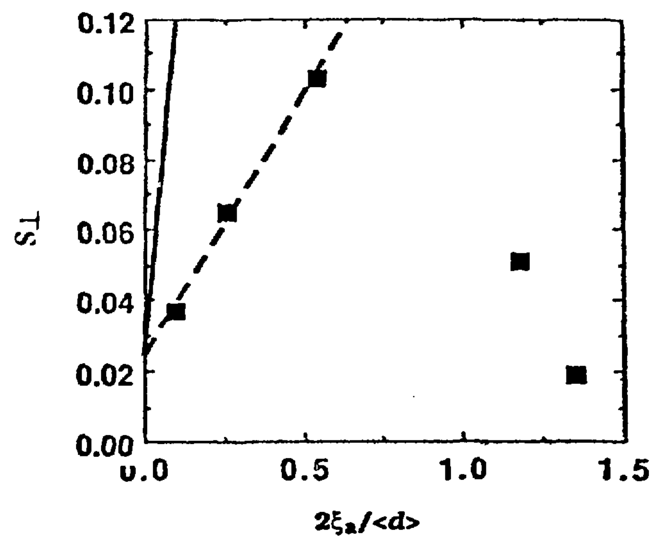

Figure 3. The dimensionless pinning force, $S_\perp$, for perpendicular fields as a function of the inverse of the average grain diameter, <*d*>, determined from the film thickness and Eq. 1. The first three points are for single films and a least-squares-fit is shown as the dashed line. The other data are for multilayers. The solid line is the maximum pinning force calculated from Eq. 5 for an *ideal* planar vacuum interface.

The single films in a parallel field showed very little anisotropy ($B_{c2||}/B_{c2\perp}$ varied from 0.8 to 0.9 for the thickest film) and only a small thickness dependence of $S_{||}$, because the thicknesses are so much greater than ξ_c. The results can also be fit to obtain an intercept of 0.029, which is somewhat larger than for perpendicular fields, but indicates that the *bulk* pinning in these NbN films is reasonably isotropic.

The results of multilayer films in a parallel field are of considerable interest, since such remarkable increases in $J_{c||}$ have recently been achieved[13]. Here the anisotropy was considerably greater with $B_{c2||}/B_{c2\perp}$ varying between 1.1 to 2.4 as the NbN layer thickness, d, decreased from 35 to 4 nm. The parallel field data, including individual films, are shown in Fig. 4 plotted against $2\xi_c$ divided by the *individual* layer thickness. Included for comparison are data points (open squares) for perpendicular fields, from Fig. 3, which are plotted against $2\xi_a$ divided by the average grain size, <*d*>, determined from Eq. 1. The solid triangle represents a sample, composed of 30 layers each of 7 nm NbN and 2 nm AlN with two 30 nm Cu layers in the middle and on the top[13], which exhibited the largest $J_{c||}$ at 20 T. The open triangle datum is for a sample with considerably thicker (5.7 nm) AlN layers between 5.5 nm NbN layers, and is thus not representative of the others which all had 2 nm AlN layers. For example, J_c has been consistently calculated as the average of the entire thickness of NbN *plus* AlN. This method would make $S_{||}$ artifically low, so we have multiplied $S_{||}$ by (5.5+5.7)/(5.5+2)=1.49.

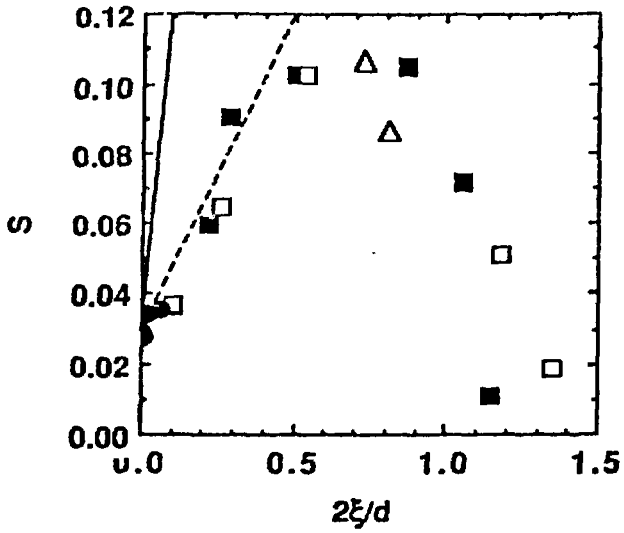

Figure 4. Compendium of the dimensionless pinning forces, S, plotted against twice the appropiate ξ divided by layer or film thickness or average grain diameter. Both parallel and perpendicular fields are included, the symbols are given in the text, and the lines are the same as Fig. 2.

The greater scatter of the parallel field data could be due to variations in the quality of the planar multilayer interfaces, the NbN quality or any misalignment of the magnetic field. The data indicate these layers have ~18% effectiveness as pinning centers, which is slightly higher than for the grain boundaries, as might be expected since the planar insulating layers should more closely approximate the ideal planar vacuum interface. The highest effectiveness is ~22%. Unfortunately this sample did not exhibit the largest $J_{c\|}$ at 20 T because B_{c2} was lower than for other multilayer samples. The largest $J_{c\|}$ at 20 T, found in the above mentioned sample with Cu layers, was primarily due to the large B_{c2} (~30 T), which is considerably greater than that of any of the other films.

The tendency for S to drop for defects smaller than 2ξ is clearly observed in Fig. 4, and is one of the primary conclusions of the experimental work. A second important conclusion involves the quantatitive comparison of the data with our model of an ideal planar vacuum interface. Although this comparison contains potential systematic errors which are hard to estimate, due, e.g., to the inadequacies of our simple model and the determination of the thermodynamic critical fields, it seems that the maximum *potential* critical depinning current density for any superconductor, J_{cm}, will occur for ideal planar vacuum interfaces spaced approximately 2ξ apart.

The excellent agreement between parallel and perpendicular field measurements shown in Fig. 4 indicates the consistency of the NbN results with uniaxial anisotropy model of the previous section.

HIGH TEMPERATURE SUPERCONDUCTORS

It is interesting to apply the above model and the results of our experiments to the new high-temperature superconductors like $YBa_2Cu_3O_7$. Assuming the pinning force is that of an ideal planar vacuum interface, it is relatively straightforward to predict the maximum *potential* J_{cm}. In Eq. 6, and its counterparts for cases II and III, we substitute[20] $B_{c2\|} \approx 230$ T, but there is some uncertainty in $B_{c2\perp}$, for B along the c-axis[20]. Using the lower value of 35 T, ξ_a/ξ_c becomes 6.5, 1 and 0.15 respectively for the three cases. The anisotropy in B_{c2} must also be included in b, but note that the validity of the $(1\text{-}b)^2$ term for fields less than $\approx B_{c2}/2$ is questionable, and J_c is usually smaller[1]. This is particularly important for B in the a-b plane, since $B_{c2} \approx 230$ T. The thermodynamic critical field, B_c, has been estimated[20] to be about 1 T in $YBa_2Cu_3O_7$.

In Eq. 6, d was replaced with $2\xi_f$, since the maximum pinning force was found to occur near there in NbN. In case I for $YBa_2Cu_3O_7$ this distance is $2\xi_c \approx 1.4$ nm, which is barely larger than the Cu-O planes spacing[22] of 0.83 nm, leading to the intriguing possibility that the intrinsic crystal structure can provide insulating layers for flux pinning. However, since $2\xi_c/d \approx 1.7$ for this situation, one expects from the results shown in Fig. 4 that the effectiveness will be significantly below the theoretical maximum predicted by Eq. 6. Two comments relate to this issue. Knowledge of ξ_c is lost[23], if the 2D nature of the Cu-O planes is reflected in $B_{c2\|}$, as was found[13] for the NbN multilayers. The spacings between Cu-O planes can be larger in other HTS, such as those based on Tl and Bi.

Ignoring any reduced effectiveness or 2D effects then Eq. 6 predicts $J_{cm}b^{1/2}/(1\text{-}b)^2$ to be, in units of 10^8 A/cm^2, given by 6.06, 2.36 and 0.14, respectively, for the above three cases at low reduced temperature. For a field of 20 T, this corresponds to J_{cm} of 17.1, 0.58 and 0.4, but note that in the first and third cases, $b \approx 0.09$, so these numbers are likely to be overestimates. Choosing instead b=0.5 provides a conservative lower limit of 2.1 and 0.05 for these cases, since J_c is a monotonic function of B. The highest value occurs for case I, with both B and J in the a-b plane, and gives $J_{cm} \geq 2\times10^8$ A/cm^2 for $B \leq 20$ T.

Note however, that another limit on J_c is the *depairing* critical current density, which is calculated[21] to be $J_{cd}=4B_c/3\sqrt{6}\mu_o\lambda_L$. Since λ_L is also anisotropic[20] in $YBa_2Cu_3O_7$, we find different values for $J_{cd}/(1\text{-}b)^2$, in units of 10^8 A/cm^2, of 0.54 and 4.7, for currents along the c-axis and in the a-b plane, respectively. This leads to J_{cd} values at 20 T for the three cases considered above of 3.9, 0.86 and 0.45, respectively, in units of 10^8 A/cm^2. These are greater than the limiting J_{cm} calculated above for 20 T, as was already suggested by Eq. 7, so that depinning and not depairing is expected to be the ultimate limit on J_c.

The effect of thermal fluctuations is expected to be much greater in HTS, because the small coherence volume, $\sim(2\xi)^3$, and large temperatures more than offset the larger condensation energy per unit volume, $B_c^2/2\mu_o$. Such fluctuations can lead to flux creep[24] and a lowering of the effective J_c below the limit calculated above for flux pinning. Since such effects are time or frequency dependent, they are complicated to quantify and further experimentation is required.

SUMMARY AND CONCLUSIONS

We have demonstrated a method to isolate flux pinning effects in measurements of J_c from the effects of changes in B_{c2} and the superconducting condensation energy, represented by T_c. This method together with microstructurally modified samples of NbN have allowed us to make an insightful experimental study of grain boundary and planar surface pinning. We show that the $(1-b)^2$ dependence of J_c on field is not restricted to a shear model of flux pinning. We also found a dramatic drop in the pinning force for each type of defect when their spacing is smaller than the flux core diameter. Based on this result and the planar vacuum interface model, we have predicted the maximum attainable J_c due to flux pinning and have shown it to be less than the maximum depairing J_c and thus the relevant ultimate limit on J_c.

For NbN columnar grain boundaries and multilayer surfaces, we find the effective pinning to be, respectively, 15% and ~18% of the theoretical maximum value for an ideal planar vacuum interface. In one case of a multilayer film we found a pinning force which was ~22% of the maximum. The analysis of these results required development of a model which also accounts for the intrinsic superconducting anisotropy of these materials and structures. However, for these structurally anisotropic single NbN films, with definite columnar grains, we found that the 'bulk' pinning, i.e., not due to surfaces of grain boundaries, was isotropic but has a value of only about 3% of the theoretical maximum. These results, taken together, give a consistent picture of pinning for the well-defined, high-pinning microstructures found in our NbN films and multilayers.

The model is also applied to the high-temperature superconductors, like $YBa_2Cu_3O_7$, to predict the maximum potential critical current density. For the case in which the field and current are parallel to the Cu-O planes, we find a value of $J_{cm} \geq 2x10^8$ A/cm^2 for $B \leq 20$ T which is less than the limit imposed by the critical *depairing* current density. However, the effects of fluctuations may be large in HTS and have been ignored in this estimate. We also point out the possibility that the intrinsic crystal structure can provide insulating layers for flux pinning.

From a practical point of view for NbN films measured in fields near 20 T, we have shown that reducing the thickness to control grain growth yields a factor of two or more increase in $J_{c\perp}$, for perpendicular applied fields, but has a much smaller effect on $J_{c||}$, for parallel applied fields. Much more significant improvements in $J_{c||}$ at 20 T have been obtained for NbN/AlN multilayer structures for which an order of magnitude increase has been achieved[13]. Such an improvement in $J_{c||}$ will be very valuable to provide the margin of safety required in practical magnet conductors, after accounting for reduced packing factors due to the addition of normal metal stabilizer and strengthening material. In addition, it should be possible with the multilayer approach to make sufficiently thick conductors, to carry the currents required for large-bore magnets, while using very thin, high-$J_{c||}$ films as the basic building blocks. However, the much lower values of $J_{c\perp}$ in multilayers could result in other problems at the ends of a magnet where the field is significantly far from a parallel orientation. Future studies of strain and radiation tolerance of these multilayers are some of the next steps towards demonstrating the practicality of these new multilayer structures.

ACKNOWLEDGEMENTS

One of us (KEG) would like to acknowledge private communications with Peter Kes and informative discussions with V. Kogan, D. Larbalestier, D.O. Welch, Jan Evetts and J.R. Clem. This work was supported by the U.S. Department of Energy, Basic Energy Sciences-Materials Sciences, under contract #W-31-109-ENG-38. Additional support for JMM came from the Argonne Division of Educational Programs.

* Present Address: Supercon, Schrewsbury, MA
** Present Address: TRW, Redondo Beach, CA

REFERENCES

1. J.E. Evetts and C.J.G. Plummer, Proc. Intl. Symp. on Flux Pinning and Electromagnetic Properties of Superconductors, edited by T. Matsushita, K. Yamafuji and F. Irie (Matsukuma Press, Fukuoka, 1985) p. 146; P.H. Kes, *IEEE Trans. on Mag.* MAG-23, 1160 (1987); and D. Dew-Hughes, *IEEE Trans. on Mag.* MAG-23, 1172 (1987).

2. K.E. Gray, R.T. Kampwirth, J.M. Murduck and D.W. Capone II, *Physica* C152, 445 (1988).

3. E.J. Kramer, *J. Appl. Phys.* 44, 1360 (1973).

4. P. Kes, private communication.

5. A.M. Campbell and J.E. Evetts, *Adv. Phys.* 21, 199 (1972), p. 412.

6. A. Pruymboom, W.H.B. Hoondert, H.W. Zandbergen and P.H. Kes, *Japan. J. Appl. Phys.* 26, 1529 (1988).

7. J.R. Gavaler, M.A. Janocko, A. Patterson and C.K. Jones, *J. Appl. Phys.* 42, 54 (1971).

8. R.T. Kampwirth, D.W. Capone II, K.E. Gray and A. Vicens, *IEEE Trans. on Mag.* MAG-21, 459 (1985).

9. D.W. Capone II, R.T. Kampwirth and K.E. Gray, *Adv. Cryogenic Engin.* 32, 659 (1985).

10. D. Dew-Hughes and R. Jones, *Appl. Phys. Lett.* **36**, 856 (1980); P. Gregshammer, H.W. Weber, R.T. Kampwirth and K.E. Gray, *J. Appl. Phys.* **64**, 1301 (1988).

11. J.W. Ekin, J.R. Gavaler and J. Gregg, *Appl. Phys. Lett.* **41**, 996 (1982).

12. H.L. Ho, R.T. Kampwirth, K.E. Gray, D.W. Capone II and L.S. Chumbley, *Ultramicroscopy* **22**, 297 (1987).

13. J.M. Murduck, D.W. Capone II, I.K. Schuller, S. Foner and J.B. Ketterson, *Appl. Phys. Lett.* **52**, 504 (1988).

14. J.M. Murduck, J. Vicent, I.K. Schuller and J.B. Ketterson, *J. Appl. Phys.* **62**, 4216 (1987).

15. C. Geibel, H. Rietschel, A. Junod, M. Pelizzone and J. Muller, *J. Phys. F: Met. Phys.* **15**, 405 (1985).

16. P.H. Kes, J. van den Berg, C.J. van der Beek, J.A. Mydosh, L.W. Roeland, A.A. Menovsky, K. Kadowaki and F.R. de Boer, *Proc. Latin American Conf. on High T_c Superconductors*, Rio de Janeiro, Brazil, May, 1988.

17. D.C. Larbalestier, in Superconductor Materials Science, edited by S. Foner and B.B. Schwartz (Plenum, New York, 1981), p. 133.

18. A.A. Abrikosov, *Zh. Eksperim. i Teor. Fiz.* **32**, 1442 (1957); *Soviet Phys. JETP* **5**, 1174 (1957), and also A.L. Fetter and P.C. Hohenberg, in Superconductivity, edited by R.D. Parks, (Marcel Dekker, New York, 1969), p.851.

19. H. Ullmaier, Irreversible Properties of Type II Superconductors, (Springer-Verlag, Berlin, 1975).

20. A. Umezawa, G.W. Crabtree, J.Z. Liu, in Proc. Intl. Conf. on High Temperature Superconductors and Materials and Mechanisms of Superconductivity edited by J. Mueller and J.L. Olsen, (North-Holland, Amsterdam, 1988) p. 1461.

21. M. Tinkham, Introduction to Superconductivity, (McGraw-Hill, New York, 1975), p. 117.

22. M.A. Beno, L. Soderholm, D.W. Capone II, D.G. Hinks, J.D. Jorgensen, J.D. Grace, I.K. Schuller, C.U. Segre and K. Zhang, *Appl. Phys. Lett.* **51**, 57 (1987).

23. J. Kang, R.T. Kampwirth and K.E. Gray, *Appl. Phys. Lett.* **52**, 2080 (1988).

24. Y. Yeshurun and A. Malozemoff, *Phys. Rev. Lett.* **60**, 2202 (1988).